J. Fluid Mech. (1990), *vol.* 214, *pp.* 639–663
Printed in Great Britain

Brownian motion far from equilibrium: a hypersonic approach

By P. RIESCO-CHUECA AND J. FERNÁNDEZ DE LA MORA
Yale University, Department of Mechanical Engineering, PO Box 2159 Y.S., New Haven, CT 06520, USA

(Received 17 November 1987 and in revised form 9 November 1989)

An investigation is carried out on the effects of Brownian agitation in the motion of small particles in a carrier gas in situations far from equilibrium. Although the standard near-equilibrium closure of the hydrodynamic equations is not valid for the heavy particles, the smallness of their speed of thermal agitation allows an alternative systematic hypersonic closure. The hypersonic equations are solved for two known instances where the kinetic Fokker–Planck equation describing the non-equilibrium particle distribution function admits exact solutions. These problems are characterized by a null or a spatially constant value for the gradient of the velocity field in the carrier gas, both being free from boundary surfaces. In the first case, where the background velocity is uniform, a fundamental solution (expressed as an integral) is obtained for the steady flow of particles from a point source; this result has obvious applications for the description of the Brownian broadening of particle streamlines. An asymptotic integration of the fundamental solution yields analytical expressions for the particle hydrodynamic properties valid everywhere except near the source, where a direct integration of the Vlasov equation completes the description. The exact solution for the second example, where the background velocity field gradient is uniform, is taken from the literature. Once these reference solutions have been established, the hypersonic equations are attacked by a variety of methods. In particular, for the uniform steady flow, a boundary-layer analysis yields analytical results identical to those obtained from the asymptotic evaluation of the kinetic fundamental solution. In both problems, the agreement found between kinetic and hydrodynamic solutions is excellent even for values of order one of the inverse particle Mach number, the expansion parameter of the hypersonic theory.

1. Introduction

The motion of Brownian particles highly diluted in a background gas, and much smaller than any macroscopic length of the problem, can be described by making use of the standard diffusion equations only under near-equilibrium conditions. In far-from-equilibrium situations the problem must be analysed within the substantially more complex framework of a kinetic theory. The inadequacy of the continuum results has already been pointed out by Einstein (1908) for the problem of a pulse of particles suddenly injected in a fluid, a situation where a non-equilibrium relaxation arises initially and lasts several particle relaxation times τ (see (2) for its precise definition). A more complete description of the kinetics of a pulse of Brownian particles injected at time zero into a quiescent fluid was given by Chandrasekhar (1943) based on the kinetic Fokker–Planck equation. This equation was also used by Kramers (1940) to describe diffusion in a harmonic potential and across the peak of a potential barrier, a problem where non-equilibrium phenomena arise when the spatial gradient of the acceleration field (the curvature of the potential) becomes comparable with the inverse square of the particle relaxation time τ. Brownian motion may thus occur within the kinetic regime either in initial or boundary layers where particles are injected or absorbed, or as the result of sufficiently inhomogeneous or rapidly varying force fields.

A problem analogous to that in which the particles are driven by an external field arises when they are carried within a given fluid velocity field $\boldsymbol{V}(\boldsymbol{x},t)$, whereupon they are subject to a viscous acceleration in the direction of their velocity relative to $\boldsymbol{V}$. Under those conditions, non-equilibrium effects occur when the product of τ with either the fluid velocity gradient or a frequency characteristic of the time variation of $\boldsymbol{V}$ is not negligible (Fernández de la Mora & Rosner 1982). Such a circumstance is often of practical interest, arising when the particles are sufficiently massive to be strongly decoupled from the fluid motion (a situation incompatible with the notion of equilibrium), but not so large for their Brownian motion to be completely negligible. Problems of inertial impaction where an aerosol suspension encounters a solid obstacle and the particles have enough inertia to collide against it with finite velocities are typical of this behaviour (Friedlander 1977, Chapter 4). Of particular interest to us is also the problem where the particles in a dusty gas are aerodynamically focused by acceleration through an axisymmetric converging nozzle and concentrated into a focal region much narrower than the exit area of the nozzle (Fernández de la Mora & Riesco-Chueca 1988). In this case, Brownian diffusion sets limits to the minimum focal width attainable, in analogy with the phenomenon of optical diffraction.

Keeping these practical problems in mind, the objective of this paper is to describe several instances of exactly solvable problems of non-equilibrium Brownian motion and to compare them with the results of an approximate hypersonic method of solution which exploits the smallness of the particles' thermal velocity relative to their mean convective speed (Freeman 1967; Freeman & Grundy 1968; Hamel & Willis 1966; Edwards & Cheng 1966; Fernández-Feria 1989). The problems will be attacked at the kinetic level by means of the well known Fokker–Planck (F–P) equation governing the velocity distribution function $f(t,\boldsymbol{x},\boldsymbol{u})$ of the heavy particles,

$$\frac{\partial f}{\partial t}+\boldsymbol{u}\cdot\nabla f=\tau^{-1}\nabla_u\cdot\left[(\boldsymbol{u}-\boldsymbol{W})f+\frac{kT}{m_p}\nabla_u f\right], \tag{1}$$

which holds for both heavy molecules and Brownian particles, under a broad range of conditions described elsewhere (Resibois & DeLeener 1977; Wang Chang & Uhlenbeck 1970; Fernández de la Mora & Fernández-Feria 1987). In (1) τ is the particle relaxation time, related to the mixture diffusion coefficient D through Einstein's law

$$D=\frac{kT\tau}{m_{\mathrm{p}}}, \tag{2}$$

where k is the Boltzmann constant, T the absolute temperature of the carrier gas, m_{p} is the mass of the particle and $\boldsymbol{W}$ is the sum of the mean velocity of the light gas $\boldsymbol{U}$ and the thermophoretic drift velocity, proportional to the gradient of temperature through the mixture thermal diffusion ratio α_T:

$$\boldsymbol{W}=\boldsymbol{U}+D\alpha_T\nabla\ln T.$$

Because a direct solution of the F–P equation is rarely feasible, other approximate techniques of solution have been implemented. Mild non-equilibrium situations where the particle partial pressure $\boldsymbol{P}_p$ is still approximately isotropic can be treated at a hydrodynamic level by adding an inertial drift term to the usual Fick diffusion term relating the velocity of the two components (Fernández de la Mora & Rosner 1982):

$$U_p = U - D\nabla \ln \rho_p - \tau(U \cdot \nabla)\, U,$$

where U_p and ρ_p are the particle mean velocity and density. This additional drift is nearly equivalent to the pressure diffusion term in the standard first-order Chapman–Enskog theory. But the expression is restricted to small values of $\tau\nabla U$, or equivalently, of the so-called Stokes number, or inertia parameter

$$S = \tau/t_f,$$

where t_f is a characteristic time of the flow. Beyond the range of small S, the pressure tensor becomes non-isotropic and the problem enters fully into the kinetic regime.

The problem may also be attacked numerically via Brownian dynamics simulations based on the equivalent stochastic Langevin equation. The technique is demanding computationally, but far less so than standard Monte Carlo simulations, and Gupta & Peters (1986) have successfully used it to describe the rates of particle collection on spherical targets under the simultaneous action of inertia and Brownian motion. The most complete results using such simulation are due to O'Brien (1990), who has computed particle densities, velocities and transitional temperatures in excellent agreement with our own analytical expressions ((17) below).

An alternative approximate procedure, which does not require such specialized numerical methods, is supplied by truncating the moment equations derived from the Boltzmann (or F–P) equation. Interestingly enough, whenever the mean convective velocity of the particles far exceeds their speed of thermal agitation, this reduction can be carried out systematically within a hypersonic theory containing the effects of Brownian motion. The problems discussed below provide a testing ground for the hypersonic expansion method and give insight about its range of applicability. A detailed account of the hypersonic approach to the F–P or the Boltzmann equation† for mixtures has been given by Fernández-Feria (1989) together with comparison of its results with exact solutions or experiments for one-dimensional problems (Fernández-Feria & Fernández de la Mora 1987*a*, *b*; Riesco-Chueca, Fernández-Feria & Fernández de la Mora 1986). The first three moment equations of the F–P equation can be expressed as

$$\frac{\partial n_p}{\partial t} + \boldsymbol{\nabla} \cdot (n_p\, U_p) = 0, \tag{3}$$

$$\frac{\partial (n_p\, U_p)}{\partial t} + \boldsymbol{\nabla} \cdot \left(n_p\, U_p\, U_p + \frac{1}{m_p} \boldsymbol{P}_p \right) = n_p \frac{1}{\tau} (\boldsymbol{W} - U_p), \tag{4}$$

$$\frac{\partial \boldsymbol{P}_p}{\partial t} + \boldsymbol{\nabla} \cdot (2\boldsymbol{Q}_p + U_p \boldsymbol{P}_p) + (\boldsymbol{P}_p \cdot \boldsymbol{\nabla})\, U_p + [(\boldsymbol{P}_p \cdot \boldsymbol{\nabla})\, U_p]^{\mathrm{T}} = \frac{2 n_p k}{\tau} (T\boldsymbol{I} - \boldsymbol{T}_p), \tag{5}$$

† This hypersonic closure for mixtures differs from the pioneering work of Hamel & Willis (1966) and Edwards & Cheng (1966) for pure gases in being applied only to the heavy component. Exploiting the fact that the relaxation scales differ widely for both components, the light gas is taken to be in equilibrium. Precedents of hypersonic closures in gas mixtures with large mass disparity may be found in Willis & Hamel (1967), Harris & Bienkowsky (1970) and Fernández-Feria & Fernández de la Mora (1987*a*, *b*), among others. None of the earlier studies incorporated the effects of Brownian motion in the direction perpendicular to the particle streamlines.

where n_p, $\boldsymbol{U}_p$, $\boldsymbol{P}_p$ and $\boldsymbol{Q}_p$ correspond to the usual hydrodynamic quantities (number density, velocity, pressure and heat flux) of the particle phase. $\boldsymbol{P}_p$ and $\boldsymbol{Q}_p$ are defined in a reference system moving locally with velocity $\boldsymbol{U}_p$.

The smallness of the heavy-species thermal velocity compared to its mean velocity is exploited by Fernández-Feria (1989) to expand (3)–(5) in powers of the mass ratio $m/m_p \ll 1$, yielding the following equations:

$$\frac{\partial \lambda_p}{\partial t} + (\boldsymbol{U}_p \cdot \nabla)\,\lambda_p + \nabla \cdot \boldsymbol{U}_p = 0, \tag{6}$$

$$\frac{\partial \boldsymbol{U}_p}{\partial t} + (\boldsymbol{U}_p \cdot \nabla)\,\boldsymbol{U}_p + \frac{k}{m_p}\{(\boldsymbol{T}_p \cdot \nabla)\,\lambda_p + \nabla \cdot \boldsymbol{T}_p\} = \frac{1}{\tau}(\boldsymbol{W} - \boldsymbol{U}_p), \tag{7}$$

$$\frac{\partial \boldsymbol{T}_p}{\partial t} + (\boldsymbol{U}_p \cdot \nabla)\,\boldsymbol{T}_p + (\boldsymbol{T}_p \cdot \nabla)\,\boldsymbol{U}_p + [(\boldsymbol{T}_p \cdot \nabla)\,\boldsymbol{U}_p]^{\mathrm{T}} = \frac{2}{\tau}(T\boldsymbol{I} - \boldsymbol{T}_p), \tag{8}$$

where $\boldsymbol{T}_p = m_p \boldsymbol{P}_p / k\rho_p$ and $\lambda_p = \ln(\rho_p/\rho_{p0})$ (ρ_{p0} is a constant reference density). Equations (6)–(8) depart from (3)–(5) only through the neglect of the heat flux tensor $\boldsymbol{Q}_p$ in the energy equation. It can be proven (Fernández-Feria 1989) that, in the absence of singularities, the results of solving (6)–(8) differ from the actual values ρ_p^e, $\boldsymbol{U}_p^e$, $\boldsymbol{T}_p^e$ (the e standing for *exact*) in quantities inversely proportional to the heavy-gas Mach number ($M_p = U_p/(kT_p/m_p)^{\frac{1}{2}}$):

$$\rho_p = \rho_p^e + O(M_p^{-3}); \quad \boldsymbol{U}_p = \boldsymbol{U}_p^e + O(M_p^{-3}); \quad \boldsymbol{T}_p = \boldsymbol{T}_p^e + O(M_p^{-1}). \tag{9}$$

If initially the heat flux tensor vanishes, the errors involved are even smaller ($O(M_p^{-4})$ for the density and velocity; $O(M_p^{-2})$ for the temperature). Notice also that, because the carrier gas molecules have a mass m typically much smaller than m_p, $m_p/m \gg 1$, the condition of hypersonicity $M_p \gg 1$ is compatible with moderately subsonic light-gas flows.

The closed system of equations (6)–(8) will be referred to throughout the paper as the hydrodynamic hypersonic equations (HH).

2. Steady expansion of a jet of particles from a point source into a uniform background gas

2.1. *Description of the problem and fundamental steady solution*

In this section an ideal point source with an output rate n' particles/s is considered, where the particles are radiated at the source with a Maxwellian velocity distribution function $\mathscr{M}(\boldsymbol{U}_0, T_0)$ with a mean velocity $\boldsymbol{U}_0$ and a temperature T_0. The background gas is moving at a uniform speed $\boldsymbol{U}_b$ in the same direction as the seeded particles and is at a uniform temperature T_b. The origin of coordinates is placed at the source, while the x-axis points in the direction of $\boldsymbol{U}_0 = U_0\,\boldsymbol{e}_x$. In what follows, a cylindrical coordinate system with axis pointing along $\boldsymbol{e}_x$ is used; the radial coordinate is denoted y, while $\boldsymbol{e}_y$ is the corresponding unit vector pointing away from the x-axis and $\boldsymbol{e}_z$ refers to the unit vector in the azimuthal direction. In §2.5 the description is extended to the two-dimensional problem (infinitely long straight-line source) where Cartesian coordinates are used: the x-axis is in the direction of $\boldsymbol{U}_0$, the z-axis is coincident with the source and the y-axis is perpendicular to x and z.

Under the assumptions $\rho_p/\rho \ll 1$, $m/m_p \ll 1$, the problem is described by (1) with $\boldsymbol{W} = \boldsymbol{U}_b$, $T = T_b$ after dropping the unsteady term $\partial f_p/\partial t$. A direct solution of this equation does not exist; but an integral representation can be obtained (similar approaches, sometimes referred to as Green-function methods are used, for instance, by Nguyen & Andres (1981) and Menon, Kumar & Sahni (1986)):

$$f_{\mathrm{p}} = n' \int_{-\infty}^{t} f_{\mathrm{F}}(t-t_0)\,\mathrm{d}t_0 = n' \int_{0}^{\infty} f_{\mathrm{F}}(t)\,\mathrm{d}t, \tag{10}$$

where $f_{\mathrm{F}}(t)$ (fundamental solution) corresponds to the evolution in time of an initial pulse injected at $t = 0$ in $\boldsymbol{x} = 0$, particles being injected at the source with the same Maxwellian velocity distribution function $\mathscr{M}(\boldsymbol{U}_0, T_0)$ and unit number density. The steady problem is thus described as a superposition of transients. The following paragraphs are devoted to the fundamental solution f_{F}.

The expression for f_{F}, given by Nguyen & Andres (1981) is an extension of previous results obtained by Chandrasekhar (1943) for the much simpler case of an initial Delta-function velocity distribution. For reasons which will become evident subsequently it is convenient to display its structure together with the equations coupling the various functions involved. The basic idea is to try a Maxwellian distribution for f_{F} with number density n_{F}, mean velocity $\boldsymbol{U}_{\mathrm{F}}$ and temperature T_{F}, such that

$$\ln n_{\mathrm{F}} = A(s) + \lambda_1(s)\,[\boldsymbol{r} - x_0(s)\,\boldsymbol{e}_x]^2; \tag{11a}$$

$$\boldsymbol{U}_{\mathrm{F}} = \boldsymbol{e}_x\,u_0(s) + [\boldsymbol{r} - x_0(s)\,\boldsymbol{e}_x]\,v_0(s); \tag{11b}$$

$$\boldsymbol{T}_{\mathrm{F}} = \theta(s)\,\boldsymbol{I}, \tag{11c}$$

where $s = t/\tau$, $\boldsymbol{r}$ is the position vector, $\boldsymbol{I}$ is the unit tensor, and the other magnitudes have been replaced by their dimensionless counterparts as follows:

$$n \leftarrow \frac{n}{(U_{\mathrm{b}}\tau)^3}, \quad \boldsymbol{U} \leftarrow \frac{\boldsymbol{U}}{U_{\mathrm{b}}}, \quad \boldsymbol{T} \leftarrow \frac{\boldsymbol{T}}{T_{\mathrm{b}}}, \quad \boldsymbol{r} \leftarrow \frac{\boldsymbol{r}}{(U_{\mathrm{b}}\tau)}, \quad f \leftarrow \frac{f}{(U_{\mathrm{b}}^2\tau)^3}. \tag{12}$$

Defining the parameter $\epsilon_{\mathrm{b}}^2 = 2kT_{\mathrm{b}}/m_{\mathrm{p}}U_{\mathrm{b}}^2$, which describes the degree of hypersonicity, and inserting the resulting Maxwellian

$$f_{\mathrm{F}} = n_{\mathrm{F}}(\pi\epsilon_{\mathrm{b}}^2 T_{\mathrm{F}})^{-\frac{3}{2}} \exp\left[-(\boldsymbol{U} - \boldsymbol{U}_{\mathrm{F}})^2/(\epsilon_{\mathrm{b}}^2 T_{\mathrm{F}})\right]$$

in the F–P equation, three differential equations for n_{F}, $\boldsymbol{U}_{\mathrm{F}}$ and T_{F} are obtained. As could be expected, they correspond to the three first moment equations (continuity, momentum and energy) with the particularity that, as a result of the symmetry of the Maxwellian distribution, no heat flux term appears in the energy equation. Therefore, for this particular example, the known solution for the complete time-dependent initial source problem coincides exactly with the hypersonic solution (equations (6)–(8)) to that same problem. The equations one obtains are

$$x_0' - u_0 = 0, \quad A' + 3v_0 = 0, \tag{13a, b}$$

$$\lambda_1' + 2v_0\lambda_1 = 0; \quad v_0' + v_0 + v_0^2 + 2\theta\lambda_1 = 0; \tag{13c, d}$$

$$\theta' + 2(\theta v_0 + \theta - 1) = 0, \tag{13e}$$

where primes denote derivatives with respect to $s = t/\tau$.

It would appear from (13*a*–*e*) that the problem is hydrodynamically closed, as one might be tempted to start the integration from initial conditions obtained by equating f_{F} at time $s = 0$ to the seeding Maxwellian distribution $\mathscr{M}(\boldsymbol{U}_0, T_0)$. It is important, however, to draw the line between the seeding distribution, which indicates the velocity statistics of the particles irradiated at the source, and the actual particle distribution function in the immediate vicinity of the source. The

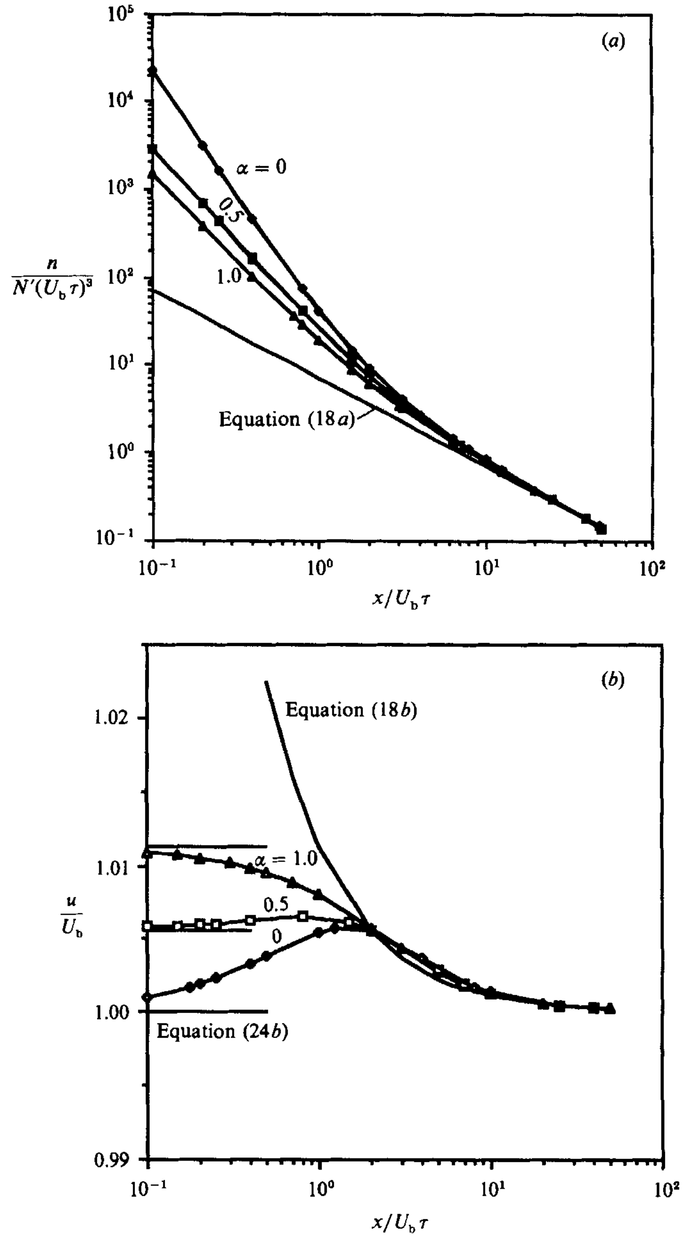

FIGURE 1 (a, b). For caption see facing page.

initial conditions for the integration of (13) have to be obtained from a local kinetic analysis at the source, closely parallel to the analysis carried out later in §2.3. Some of the variables (v_0, A) turn out to be singular at $s = 0$, while the initial condition for θ ($\theta(0) = 0$) bears no connection to the initial temperature T_0 of the seeded particles. Details are not given, but it can be verified that (13) are indeed satisfied by the actual solution:

$$u_0 = 1 + \delta\,\mathrm{e}^{-s}; \quad x_0 = s + \delta b; \quad A = -\tfrac{3}{2}\ln(\pi\epsilon_b^2\, a), \tag{14a–c}$$

$$v_0 = c/a; \quad \theta = d/a; \quad \lambda_1 = -1/(a\epsilon_b^2), \tag{14d–f}$$

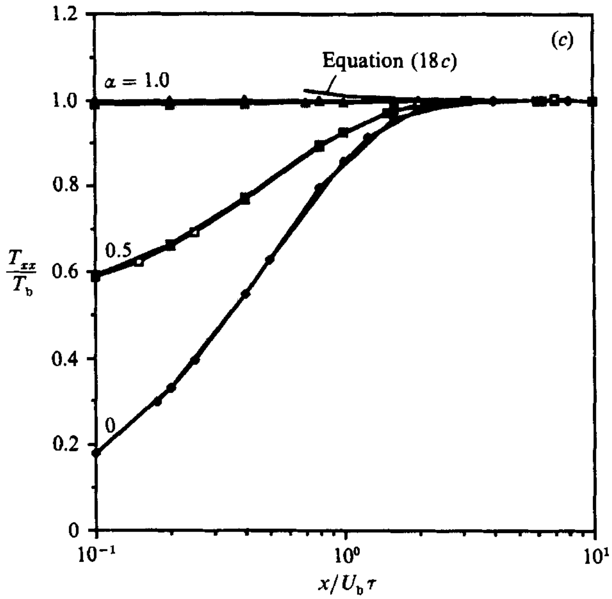

FIGURE 1. Profiles of (*a*) the particle density, (*b*) axial velocity and (*c*) axial temperatures ($n/N'(U_b\tau)^3$, u/U_b, T_{xx}/T_b as a function of $x/U_b\tau$) along the axis in the point-source expansion problem, for $\delta = 0$ (i.e. $U_0 = U_b$) and different values of $\alpha = T_0/T_b$ ($\epsilon_b = 0.15$ and $N' = 1$: $\triangle$, $\alpha = 1$; $\square$, $\alpha = 0.5$; $\diamond$, $\alpha = 0$), as obtained from the numerical integration of the F–P equation. The far-field near-equilibrium solution (equation (18)) is also plotted for large values of $x/(U_b\tau)$, as well as the asymptotic Laplace integration results given in (27), (28) and (50) (solid symbols). In (*b*), the Vlasov approximation for the velocity (equation (24*b*)) is also represented for small values of $x/(U_b\tau)$. The agreement between numerical and asymptotic integration of the F–P equation is equally good for other values of δ.

where the functions $a(s)$, $b(s)$, $c(s)$ and $d(s)$ are given by

$$b = 1-e^{-s}, \quad a = \alpha b^2+2s-3-e^{-2s}+4e^{-s}, \quad c = \tfrac{1}{2}a' = b(1-e^{-s}+\alpha e^{-s}), \tag{15a–c}$$

$$d = \alpha[1-4e^{-s}+(2s-3)e^{-2s}]+2s-4+8e^{-s}-(2s+4)e^{-2s}, \tag{15d}$$

while the constants α and δ are related to the initial conditions of the seed particles:

$$\alpha = T_0/T_b, \quad \delta = (U_0-U_b)/U_b. \tag{16}$$

Alternatively, the evaluation of f_F can be carried out at a strictly kinetic level, following Chandrasekhar (1943) in the application of the method of characteristics to the Fourier transform of the F–P equation. In that way, the structure of the solution results naturally from the characteristic invariants.

Once the fundamental solution f_F is known one can turn back to the steady problem and determine the particle phase hydrodynamic magnitudes n, $\boldsymbol{U} = u\boldsymbol{e}_x+v\boldsymbol{e}_y$ and $\boldsymbol{T} = T_{xx}\boldsymbol{e}_x\boldsymbol{e}_x+T_{yy}\boldsymbol{e}_y\boldsymbol{e}_y+T_{zz}\boldsymbol{e}_z\boldsymbol{e}_z+T_{xy}(\boldsymbol{e}_x\boldsymbol{e}_y+\boldsymbol{e}_y\boldsymbol{e}_x)$ (from symmetry considerations, T_{xz} and T_{yz} are zero) by using their definitions based on integrals of f_p in velocity space and interchanging the order of velocity and time integration. In terms of n_F, $\boldsymbol{U}_F$ and $\boldsymbol{T}_F$ as defined in (11) one obtains

$$n = N'\int_0^\infty n_F\,ds, \quad n\boldsymbol{U} = N'\int_0^\infty n_F\,\boldsymbol{U}_F\,ds, \tag{17a, b}$$

$$\boldsymbol{T} = \frac{2}{\epsilon_b^2}\left\{\frac{N'}{n}\int_0^\infty n_F\, \boldsymbol{U}_F\, \boldsymbol{U}_F\, \mathrm{d}s - \boldsymbol{U}\boldsymbol{U}\right\} + \boldsymbol{I}\frac{N'}{n}\int_0^\infty n_F\, T_F\, \mathrm{d}s, \tag{17c}$$

where $N' = n'\tau$ and the same normalization as introduced in (12) is used. The above integration leading to n, $\boldsymbol{U}$ and $\boldsymbol{T}$ can be carried out numerically. Figure 1 (a–c) shows the n, $\boldsymbol{U}$ and T_{xx} profiles along the axis for different values of α and $\delta = 0$ (equation (16)) in the case where $\epsilon_b = 0.15$ and $N' = 1$. In the following paragraphs, some particular cases or regions of the flow will be thoroughly analysed and compared later with results from the HH equations.

2.2. *Far field* ($r \gg U_b\tau, r \gg U_0\tau$)

In this limit most of the contribution to the integrals (17) comes from pulses radiated far back in time. This feature opens the door to an asymptotic integration scheme in which the functions a, b, c and d are approximated by the leading term of their polynomial expansion for $s \gg 1$, and the resulting integrals, which turn out to be analytically solvable, are carried out to yield

$$n = \frac{N'}{2\pi\epsilon_b^2\, r}\exp\left(\frac{-(r-x)}{\epsilon_b^2}\right), \tag{18a}$$

$$\boldsymbol{U} = \frac{1}{2}\left(\boldsymbol{e}_x + \boldsymbol{e}_r\left(1+\frac{\epsilon_b^2}{r}\right)\right), \tag{18b}$$

$$\boldsymbol{T} = \boldsymbol{I}\left(1-\frac{1}{2r}\left[1+\frac{\epsilon_b^2}{r}\right]\right) + \frac{1}{2r}\boldsymbol{e}_r\boldsymbol{e}_r\left(1+2\frac{\epsilon_b^2}{r}\right), \tag{18c}$$

where $\boldsymbol{e}_r = \boldsymbol{r}/r$ and $x = \boldsymbol{r}\cdot\boldsymbol{e}_x$. The above solution is exactly coincident with the results from a near-equilibrium hydrodynamic formulation (continuity, diffusion law, pressure tensor/viscosity relation), which in physical variables can be expressed as

$$\nabla\cdot(n_p\,\boldsymbol{U}_p) = 0, \quad \boldsymbol{U}_p - \boldsymbol{U}_b = -D\nabla\ln n_p, \quad \boldsymbol{T}_p = T_b(\boldsymbol{I} - \tfrac{1}{2}\tau(\nabla\boldsymbol{U}_p + \nabla\boldsymbol{U}_p^{\mathrm{T}})).$$

The last equation reduces to the standard Navier–Stokes form by using the relation $\mu_p = \frac{1}{2}\rho_p D$ which corresponds to an effective Schmidt number $Sc = \mu_p/\rho_p D = \frac{1}{2}$, consistent with previous values given for Sc (Fernández de la Mora 1982) in problems under the F–P assumptions (large mass disparity and dilution of the heavy species):

$$\boldsymbol{P}_p = n_p\, kT_b\,\boldsymbol{I} - \mu_p(\nabla\boldsymbol{U}_p + \nabla\boldsymbol{U}_p^{\mathrm{T}}).$$

The diffusion solution (18) is plotted in figure 1(a–c) together with the exact numerically integrated solution. The diffusion regime can be observed to set in only for distances from the source between 5 and 10.

2.3. *Vicinity of the source*

Spatial gradients are large close to the source, so that the streaming operator in the Boltzmann equation is dominant with respect to the collision term. Hence, at distances $r \ll U_0\tau$, not only is the effect of self-collisions neglected (which is a standard feature of the Fokker–Planck equation) but also that of cross-collisions. The kinetic behaviour is thus described by the so-called Vlasov equation:

$$(\boldsymbol{u}_p\cdot\nabla)f_p = 0, \tag{19}$$

according to which the distribution function is conserved along phase-space trajectories (straight lines with constant velocity). Because the background fluid properties are now irrelevant, we base the new dimensionless variables on the particle injection properties U_0, T_0, as follows:

$$n \leftarrow \frac{n}{(U_0\tau)^3}, \quad \boldsymbol{U} \leftarrow \frac{\boldsymbol{U}}{U_0}, \quad \boldsymbol{T} \leftarrow \frac{\boldsymbol{T}}{T_0}, \quad \boldsymbol{r} \leftarrow \frac{\boldsymbol{r}}{(U_0\tau)}, \quad \epsilon_0^2 = \frac{2kT_0}{m_p U_0^2}. \tag{20}$$

Obviously, this notation excludes the case $\alpha = 0$, which will be considered later. The molecules radiated at the source are distributed in velocity space according to a Maxwellian velocity distribution g_M:

$$g_M\, d^3v = (\pi\epsilon_0^2)^{-\frac{3}{2}} \exp\left(-(\boldsymbol{v}-\boldsymbol{e}_x)^2/\epsilon_0^2\right) d^3v.$$

In spherical coordinates ($u = (V, \theta, \phi)$, where V is the magnitude of the velocity, the distribution becomes

$$g_M V^2\, dV\, d\Omega_v = (\pi\epsilon_0^2)^{-\frac{3}{2}} V^2 \exp\left(-\frac{1}{\epsilon_0^2}[\sin^2\theta + (V-\cos\theta)^2]\right) dV\, d\Omega_v, \tag{21}$$

where $d\Omega_v = \sin\theta\, d\theta\, d\phi$. The marginal density function $g_\Omega \equiv \int_0^\infty g_M V^2\, dV$ gives the fraction of the total output of molecules which point in the direction specified by the solid angle element $d\Omega_v$, so that by continuity:

$$N' g_\Omega\, d\Omega = n U_r r^2\, d\Omega, \tag{22}$$

where U_r is the mean velocity in the radial direction. Upon comparison of (21)–(22) with the normal kinetic definition of the mass flow density

$$nU_r = \int f v_r\, d^3u,$$

where v_r is the molecule velocity in the radial direction, it follows that the velocity distribution function at r is

$$f = \frac{N'}{(\pi\epsilon_0^2)^{\frac{3}{2}} r^2} v_r \exp\left(-\frac{1}{\epsilon_0^2}[(v_r - \cos\theta)^2 + \sin^2\theta]\right) H(v_r)\, \delta(v_\theta)\, \delta(v_\phi), \tag{23}$$

where $H(v_r)$ is a unit step function ($H = 1$ for $v_r > 0$, $H = 0$ otherwise) and $\delta(x)$ is the Dirac distribution. According to (23), the temperature in the radial direction is of order unity while it is zero in the transverse directions, and only outflowing molecules exist close enough to the source. The hydrodynamic quantities around the source can now be obtained by integration:

$$n = \int f\, d^3v, \quad \boldsymbol{U} = \frac{1}{n}\int \boldsymbol{v} f\, d^3\boldsymbol{v}, \quad \boldsymbol{T} = \frac{2}{\epsilon_0^2 n}\int (\boldsymbol{v}-\boldsymbol{U})(\boldsymbol{v}-\boldsymbol{U}) f\, d^3v.$$

Carrying out the above integrals, exact analytical expressions are derived for n, $\boldsymbol{U}$ and $\boldsymbol{T}$ for the case where $\alpha \neq 0$:

$$n = \frac{N' \cos\theta}{2\pi\epsilon_0^2 r^2} \exp\left(-\frac{\sin^2\theta}{\epsilon_0^2}\right) \operatorname{erfc}\left(-\frac{\cos\theta}{\epsilon_0}\right)\left(1 + \frac{\epsilon_0 Q}{\cos\theta} + O(r)\right), \tag{24a}$$

$$\boldsymbol{U} = \boldsymbol{e}_r \cos\theta \frac{1 + \dfrac{3\epsilon_0 Q}{\cos\theta} + \dfrac{\epsilon_0^2}{2\cos^2\theta}}{1 + \dfrac{\epsilon_0 Q}{\cos\theta}} + O(r), \tag{24b}$$

$$\boldsymbol{T} = \boldsymbol{e}_r \boldsymbol{e}_r \frac{1 + \dfrac{3\epsilon_0 Q}{\cos\theta} + \dfrac{\epsilon_0^2}{\cos^2\theta}(2Q^2 - \frac{1}{2})}{1 + \left(\dfrac{\epsilon_0 Q}{\cos\theta}\right)^2}, \tag{24c}$$

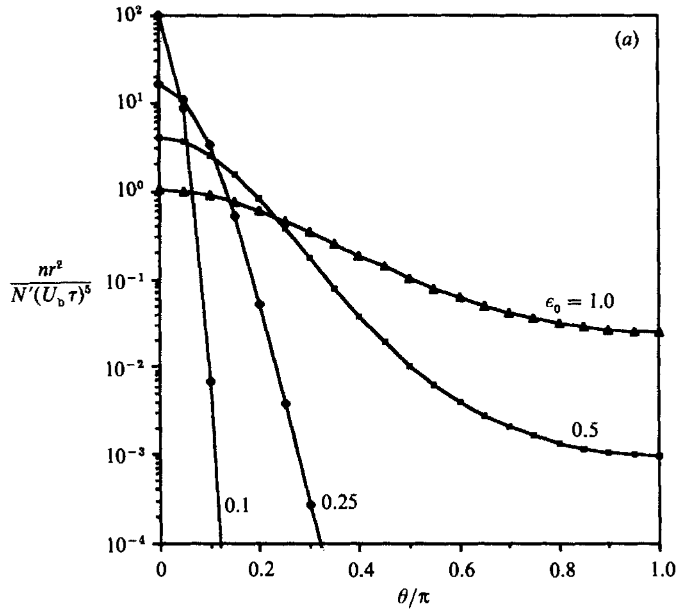

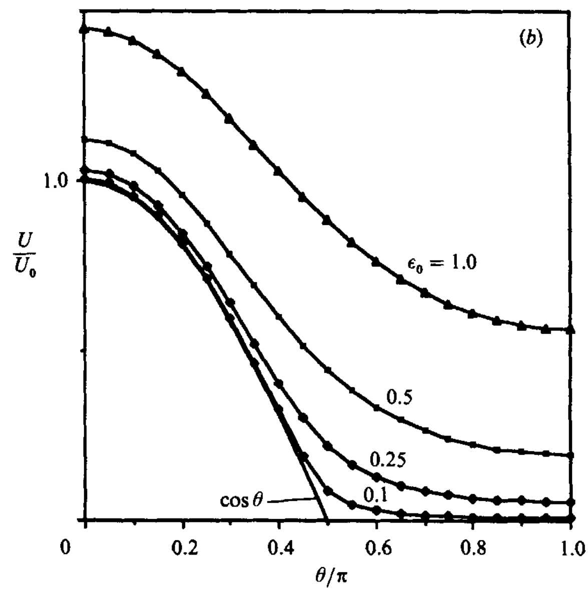

FIGURE 2(*a*, *b*). For caption see facing page.

where
$$Q = \frac{\exp(-\cos^2\theta/\epsilon_0^2)}{\pi^{\frac{1}{2}}\operatorname{erfc}(-\cos\theta/\epsilon_0)}.$$

Figure 2 shows profiles of density, velocity and radial temperature as a function of θ according to (24) for different values of ϵ_0. The density profile flattens out as ϵ_0 increases (initial Mach number decreases). In the hypersonic limit $\epsilon_0 \rightarrow 0$, the velocity tends to the function $U = \cos\theta$ ($|\theta| < \frac{1}{2}\pi$). Another interesting property of (24) is the fact that, regardless of ϵ_0, the radial temperature for $\theta = \frac{1}{2}\pi$ takes the constant value $T_0'(2-\frac{1}{2}\pi)$. It is important to note that the Vlasov analysis is not restricted to small

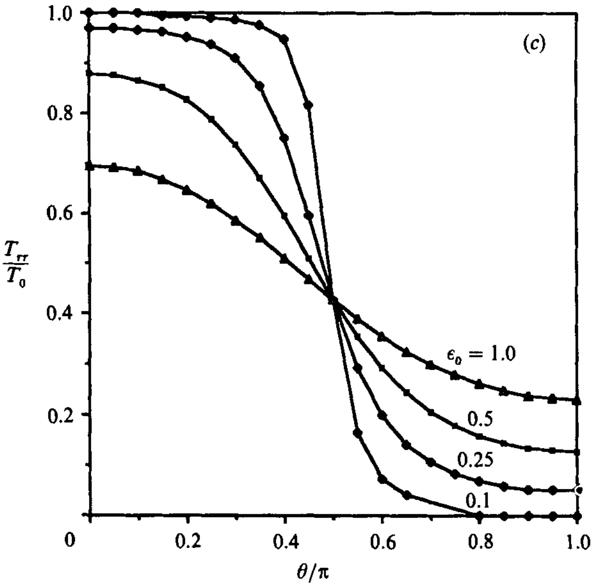

FIGURE 2. (*a*) Particle number density, (*b*) velocity and (*c*) radial temperature ($nr^2/[n'(U_0\tau)^5]$, U/U_0, T_{rr}/T_0, where $T_{rr} = \boldsymbol{e}_r \cdot \boldsymbol{T} \cdot \boldsymbol{e}_r$) very close to the source ($r \ll 1$) (see (24)) as a function of the angle θ from the seeding direction for different values of the hypersonic parameter $\epsilon_0 = 2kT_0/m_p U_0^2$ (Vlasov solution): $\epsilon_0 = 0.1$ (◆), $\epsilon_0 = 0.25$ (◇), $\epsilon_0 = 0.5$ (■), $\epsilon_0 = 1$ (△). The density is represented with a scaling factor r^2, as follows from (24*a*).

values of ϵ_0 and therefore covers a much broader range of situations than the HH analysis in the vicinity of the source.

The same conclusions could alternatively be reached by expansion in powers of s of the integrands in (17) (in the vicinity of $s = 0$, the functions a, b, c and d given in (15) can be expanded in powers of s and substituted in (14), (11) to yield integrable expressions). The result is an expansion in powers of the radial distance r, whose leading term is in exact agreement with (24).

The case of initial zero temperature, $\alpha = 0$, requires a separate treatment. The Vlasov equation does not provide any information except for the trivial result that the initial Delta distribution remains approximately unchanged close to the source. One needs to take into account the effect of cross-collisions, ignored by the Vlasov model, in order to perceive any change from the initial distribution function. On the other hand, the asymptotic integration of (17) becomes considerably more complex than in the case $\alpha \neq 0$, because the lowest-order term of the integrand's expression does not allow a direct analytical solution. However, good approximations for the integrals in (17) can be obtained by using the Laplace method discussed in the next section.

2.4. *Asymptotic integration in the hypersonic limit* $\epsilon_b \ll 1$

The integrals in (17) can be written in the general form $\int_0^\infty n_F F(s)\,\mathrm{d}s$,

$$I(F) \equiv \int_0^\infty \mathrm{d}s\, F(s)\,[\pi\epsilon_b^2\, a(s)]^{-\frac{3}{2}} \exp\left\{-\frac{[x-x_0(s)]^2+y^2}{a(s)\,\epsilon_b^2}\right\} \tag{25}$$

with $F(s) = 1$, $\boldsymbol{U}_F$, $\boldsymbol{U}_F\boldsymbol{U}_F$ and T_F, respectively. The small value of ϵ_b in the exponential term leads to a very rapid decay of the integrand around the minimum absolute value of the exponent. Evidently, particles have a negligible number density except in the region of interest where the inner variable

$$\eta_\mathrm{b} \equiv y/\epsilon_\mathrm{b}$$

takes values of order one and the factor $\exp[-\eta_\mathrm{b}^2/a(s)]$ has a slow variation. Most of the contribution to the integral occurs in the vicinity of the value s_0 of s at which

$$x_0(s_0) = x.$$

In that narrow region one may give a simplified local description of the integrand and evaluate $I(F)$ asymptotically. Defining the new independent variable

$$z(s,x) \equiv \frac{[x-x_0(s)]}{(a(s))^{\frac{1}{2}}},$$

for $x > 0$, (25) may be written asymptotically as

$$I(F) = \int_{-\infty}^{\infty} \mathrm{d}z\,(\pi\epsilon_\mathrm{b}^2)^{-\frac{3}{2}} G(z)\exp(-z^2/\epsilon_\mathrm{b}^2)$$

with $$G(z) \equiv -\frac{F(s)\exp[-\eta_\mathrm{b}^2/a(s)]}{a^{\frac{3}{2}}(s)\,z'(s)}.$$

Expanding G in Taylor series around $z = 0$ and integrating, it follows that

$$I(F) = (\pi\epsilon_\mathrm{b}^2)^{-1}\left\{G(z)+\tfrac{1}{4}\epsilon_\mathrm{b}^2\frac{\partial^2 G(z,x,\eta_\mathrm{b})}{\partial z^2}+O(\epsilon_\mathrm{b}^4)\right\}_{s=s_0}. \tag{26}$$

Naturally, this description fails in the vicinity of $x = 0$, where $a(s)$ is singular, and the proper local approximation was discussed earlier in §2.3.

To lowest order, (26) implies that

$$n_0 = N'[\pi\epsilon_\mathrm{b}^2\,a(s_0)\,u_0(s_0)]^{-1}\exp[-\eta_\mathrm{b}^2/a(s_0)], \tag{27a}$$

$$\boldsymbol{U}_0 = \boldsymbol{U}_\mathrm{F}(s_0) = u_0(s_0)\,\boldsymbol{e}_x+\epsilon_\mathrm{b}\,\eta_\mathrm{b}\,v_0(s_0)\,\boldsymbol{e}_y. \tag{27b}$$

The temperature tensor may be decomposed into two contributions, $\boldsymbol{T} = \boldsymbol{T}_\mathrm{c}+\boldsymbol{T}_\mathrm{T}$, which we shall call 'convective' and 'thermal', respectively:

$$n\boldsymbol{T}_\mathrm{c} = \frac{2}{\epsilon_\mathrm{b}^2}\{N'I(\boldsymbol{U}_\mathrm{F}\,\boldsymbol{U}_\mathrm{F})-n\boldsymbol{U}\boldsymbol{U}\}, \tag{28a}$$

$$\boldsymbol{T}_\mathrm{T} = \boldsymbol{I}I(T_\mathrm{F}) = \theta(s_0)\,\boldsymbol{I}+O(\epsilon_\mathrm{b}^2). \tag{28b}$$

Evidently, the determination of $\boldsymbol{T}$ to lowest order requires computing n, $\boldsymbol{U}$ and $I(\boldsymbol{U}_\mathrm{F}\,\boldsymbol{U}_\mathrm{F})$ correctly up to order ϵ_b^2, which involves the cumbersome calculation of $\partial^2 G/\partial z^2$. To simplify the notation we define

$$M(F) \equiv \tfrac{1}{4}\left[a u_0 \exp(\eta_\mathrm{b}^2/a)\frac{\partial^2 G}{\partial z^2}\right]_{s=s_0} \tag{29}$$

and rewrite (26) as

$$n = I(1) = n_0\{1+\epsilon_\mathrm{b}^2 M(1)\}+O(\epsilon_\mathrm{b}^4), \tag{30a}$$

$$n\boldsymbol{U} = I(\boldsymbol{U}_\mathrm{F}) = n_0\{\boldsymbol{U}_0+\epsilon_\mathrm{b}^2 M(\boldsymbol{U}_\mathrm{F})\}+O(\epsilon_\mathrm{b}^4), \tag{30b}$$

$$N'I(\boldsymbol{U}_\mathrm{F}\,\boldsymbol{U}_\mathrm{F}) = n_0\{\boldsymbol{U}_0\,\boldsymbol{U}_0+\epsilon_\mathrm{b}^2 M(\boldsymbol{U}_\mathrm{F}\,\boldsymbol{U}_\mathrm{F})\}+O(\epsilon_\mathrm{b}^4). \tag{30c}$$

Because the functions M involve double derivation of $\exp(-\eta_b^2/a)$, they are biquadratic polynomials of η_b (aside from further η_b-dependences in $F(s)$):

$$M(F) = A(F, s_0)\,\eta_b^4 + B(F, s_0)\,\eta_b^2 + C(F, s_0), \tag{31}$$

where

$$A = A_0(s)\,F; \quad B = B_0(s)\,F + B_1(s)\,F'; \quad C = C_0(s)\,F + C_1(s)\,F' + C_2(s)\,F''$$

and the following F-invariant coefficients have been introduced:

$$A_0(s) = \frac{a'^2}{4a^3u_0^2},$$

$$B_0(s) = \frac{1}{4u_0^2}\left(\frac{a''}{a} - \frac{2a'^2}{a^2} - \frac{3a'u_0'}{au_0}\right); \quad B_1(s) = \frac{a'}{2au_0^2}$$

$$C_0(s) = \frac{a}{4u_0^2}\left(\frac{3u_0'^2}{u_0^2} - \frac{u_0''}{u_0}\right); \quad C_1(s) = -\frac{3au_0'}{4u_0^3}; \quad C_2(s) = \frac{a}{4u_0^2}.$$

Notice again that the $M(F)$-functions depend on x and η_b (or y), not on s. But the x-dependence is given parametrically in terms of s_0 by $x = x_0(s_0)$. From (28a) and (30), $\boldsymbol{T}_c$ may now be expressed to lowest order in ϵ_b^2 as

$$\boldsymbol{T}_c = 2\{M(\boldsymbol{U}_F\,\boldsymbol{U}_F) + M(1)\,\boldsymbol{U}_0\,\boldsymbol{U}_0 - \boldsymbol{U}_0 M(\boldsymbol{U}_F) - M(\boldsymbol{U}_F)\,\boldsymbol{U}_0\} + O(\epsilon_b^2). \tag{32}$$

Upon substitution of (31), it follows that the term in η_b^4 is proportional to $(\boldsymbol{U}_F - \boldsymbol{U}_0)(\boldsymbol{U}_F - \boldsymbol{U}_0)$, while the term in η_b^2 is proportional to $(\boldsymbol{U}_F - \boldsymbol{U}_0)\,\boldsymbol{U}_F' + \boldsymbol{U}_F'(\boldsymbol{U}_F - \boldsymbol{U}_0)$, so that setting $s = s_0$ and recalling (27b), both terms are seen to vanish and $\boldsymbol{T}_c$ becomes

$$\boldsymbol{T}_c = 4C_2(s_0)\,\boldsymbol{U}_F'(s_0)\,\boldsymbol{U}_F'(s_0) + O(\epsilon_b^2). \tag{33}$$

Hence, using (28),

$$T_{xx} = \frac{d}{a} + a\left(v_0 - \frac{u_0'}{u_0}\right)^2 + O(\epsilon_b^2), \tag{34a}$$

$$T_{xy} = a\frac{v_0'}{u_0}\left(v_0 - \frac{u_0'}{u_0}\right)\epsilon_b\,\eta_b(1 + O(\epsilon_b^2)), \tag{34b}$$

$$T_{yy} = \frac{d}{a} + O(\epsilon_b^2), \tag{34c}$$

where, as before, the primes denote s-derivatives, and the functions a, u_0, v_0, ... are evaluated at $s = s_0$, where s_0 is defined implicitly by the equation $x_0(s_0) = x$. The other components of the convective temperature tensor are of $O(\epsilon_b^2)$ or smaller. Therefore, to lowest order, $T_{xx} = T_{cxx} + \theta$, $T_{xy} = T_{cxy}$ and $T_{yy} = T_{zz} = \theta$. For future reference, it is also convenient to obtain the next order approximation of the velocity $\boldsymbol{U}$. From (30a, b) it follows that

$$\boldsymbol{U} = \boldsymbol{U}_0 + \epsilon_b^2\,\boldsymbol{U}_1 + O(\epsilon_b^4),$$

where

$$\begin{aligned}\boldsymbol{U}_1 &= M(\boldsymbol{U}_F) - \boldsymbol{U}_0 M(1)\\ &= B_1(s_0)\,\boldsymbol{U}_F'(s_0)\,\eta_b^2 + C_1(s_0)\,\boldsymbol{U}_F'(s_0) + C_2(s_0)\,\boldsymbol{U}_F''(s_0).\end{aligned} \tag{35}$$

In figure 1(a–c), the lowest-order Laplace expressions for n, $u = U_x$ and T_{xx}, respectively given in (27a), (27b) and (14f) together with (34a), are plotted along the axis for the same example as before ($N' = 1, \epsilon_b = 0.15$). The agreement with the results from a numerical evaluation of the convolution integrals (17) is excellent both along the axis and transversally to it (not plotted). Equally satisfactory is the lowest-order approximation for $v = U_y$, T_{yy} and T_{xy} (not represented), as well as the first correction to U given in (35). The accuracy of the Laplace expressions away from the ejection axis is good, provided that the transversal coordinate does not exceed values around $\eta_b = 5$.

2.5. *Hypersonic (HH) results*

Having obtained exact expressions for the particle flow parameters, the hypersonic equations are now considered in order to test their accuracy against the kinetic standard. So far, the analysis was restricted to an axially symmetric geometry. The hydrodynamic approach allows the incorporation of the two-dimensional case in the same formulation. Let ϕ be a parameter taking the value 1 for axisymmetrical flow and 0 in the two-dimensional case. The HH equations for the steady problem are

$$\mathrm{D}\lambda + u_x + v_y + \phi v/y = 0, \tag{36a}$$

$$\mathrm{D}u + \epsilon^2(\mathrm{D}_1\lambda + T_{xx,x} + T_{xy,y} + \phi T_{xy}/y) = 1 - u, \tag{36b}$$

$$\mathrm{D}v + \epsilon^2(\mathrm{D}_2\lambda + T_{xy,x} + T_{yy,y} + \phi(T_{yy} - T_{zz})/y) = -v, \tag{36c}$$

$$\mathrm{D}T_{xx} + 2\mathrm{D}_1 u = 2(1 - T_{xx}), \tag{36d}$$

$$\mathrm{D}T_{xy} + \mathrm{D}_1 v + \mathrm{D}_2 u = -2T_{xy}, \tag{36e}$$

$$\mathrm{D}T_{yy} + 2\mathrm{D}_2 v = 2(1 - T_{yy}), \tag{36f}$$

$$\mathrm{D}T_{zz} + 2v\phi T_{zz}/y = 2(1 - T_{zz}), \tag{36g}$$

where $\epsilon^2 = kT_b/m_p U_b^2 = \frac{1}{2}\epsilon_b^2$ and the normalization defined in (12) is used, while the operators $\mathrm{D} = u\,\partial_x + v\,\partial_y$, $\mathrm{D}_1 = T_{xx}\,\partial_x + T_{xy}\,\partial_y$, $\mathrm{D}_2 = T_{xy}\,\partial_x + T_{yy}\,\partial_y$ are introduced. T_{zz} stands for the azimuthal temperature in the axisymmetrical case. For the temperature components, a comma in the subscript denotes a partial derivative with respect to the variable following the comma.

The underlying assumption for the HH equations to hold, $\epsilon^2 \ll 1$, can be further exploited to find an approximate solution to (36). In other words, the region around the axis can be considered a boundary layer where rescaled variables are introduced:

$$v = \epsilon w, \quad y = \epsilon\eta, \quad T_{xy} = \epsilon\theta_{xy}.$$

Taking into account that u depends on y only to order ϵ^2,

$$u = u_0(x) + \epsilon^2 u_1(x, \eta).$$

To lowest order one obtains ($\mathrm{d}/\mathrm{d}s = {}' = u_0\,\partial_x + w\,\partial_\eta$):

$$\lambda' + u_{0x} + w_\eta + \phi w/\eta = 0, \tag{37a}$$

$$u_0' + u_0 - 1 = 0, \tag{37b}$$

$$w' + w + T_{yy}\lambda_\eta + \phi(T_{yy} - T_{zz})/\eta = 0, \tag{37c}$$

$$T_{xx}' + 2(T_{xx} - 1 + T_{xx}u_{0x}) = 0, \tag{37d}$$

$$T_{zz}' + 2(T_{zz} - 1 + wT_{zz}\phi/\eta) = 0, \tag{37e}$$

$$\theta_{xy}' + \theta_{xy}(2 + u_{0x} + w_\eta) + T_{xx}w_x + T_{yy}u_{1\eta} = 0, \tag{37f}$$

$$u_1' + u_1 + T_{xx}\lambda_x + T_{xx,x} + \theta_{xy,\eta} + \theta_{xy}\lambda_\eta + u_1 u_{0x} + \phi\theta_{xy}/\eta = 0. \tag{37g}$$

Equation (37*b*) can be parametrically solved to obtain

$$x = s+\delta(1-e^{-s}), \quad u_0 = 1+\delta e^{-s}. \tag{38}$$

If the structure of previous results for the Laplace solution to the F–P equation is recalled, one can postulate the existence of exact solutions to (37) of the form

$$\lambda = \lambda_0(x)+\eta^2\lambda_1(x), \quad T_{xx} = \theta_{xx}(x), \quad T_{yy} = \theta(x), \quad T_{zz} = \zeta(x),$$
$$\theta_{xy} = \eta\beta(x), \quad w = \eta v_0(x), \quad u_1 = p(x)+\eta^2 q(x).$$

For functions depending only on x the notation $' = \mathrm{d}/\mathrm{d}s = u_0\,\mathrm{d}/\mathrm{d}x$ is preserved. Thus, the governing equations become

$$\lambda_0'+v_0(1+\phi)+u_0'/u_0 = 0, \tag{39a}$$

$$\lambda_1'+2v_0\lambda_1 = 0, \tag{39b}$$

$$v_0'+v_0+v_0^2+2\theta\lambda_1 = 0, \tag{39c}$$

$$\theta'+2(\theta v_0+\theta-1) = 0, \tag{39d}$$

$$\theta_{xx}'+2\theta_{xx}(1+u_0'/u_0)-2 = 0, \tag{39e}$$

$$\beta'+\beta(2v_0+2+u_0'/u_0)+\theta_{xx}v_0'/u_0+2\theta q = 0, \tag{39f}$$

$$p'+p[1+u_0'/u_0]+\theta_{xx}\lambda_0'/u_0+\theta_{xx}'/u_0+\beta(\phi+1) = 0, \tag{39g}$$

$$q'+q[1+u_0'/u_0]+2qv_0+\theta_{xx}\lambda_1'/u_0+2\beta\lambda_1 = 0, \tag{39h}$$

$$\zeta'+2(\zeta-1) = 0 \quad (\text{for } \phi = 0); \quad \zeta = \theta \quad (\text{for } \phi = 1). \tag{39i}$$

Notice that (39*b*–*d*) are identical to (13*c*–*e*) describing the time-dependent initial source problem, and that they are decoupled from the rest; their independence from ϕ indicates that the solution (14*e*–*g*) holds for two-dimensional as well as axisymmetrical situations. As before, the singularity of the problem at the source precludes a hydrodynamic closure. The boundary conditions for (39) have to be obtained from kinetic arguments; one gets $v_0 = c/a$, $\theta = d/a$, while $\lambda_1 = -1/2a$ (a different factor from the time-dependent one, because of the different normalization), where the functions a, c and d are s-dependent. This is not a real time-dependence as in the fundamental solution, but a parametric representation of the x-dependence through (38).

All the other equations are different in the two problems. In particular, the temperature is no longer a scalar in the steady case and therefore requires further equations for its complete specification. Equations (39*a*, *e*) can be separately solved:

$$\lambda_0 = -\ln[u_0 a^{(1+\phi)/2}]+\text{const}, \tag{40a}$$

$$\theta_{xx} = e^{-2s}[e^{2s}-1+\alpha(1+\delta)^2+4\delta(e^s-1)+2\delta^2 s]/u_0^2, \tag{40b}$$

where the condition $\theta_{xx}(0) = \alpha$, resulting from the kinetic (Vlasov) analysis, has been used. The remaining equations (39*f*–*h*) are coupled and no attempt has been made to find an analytic solution. It is not a surprise that the lowest-order expressions obtained with the above method for the density (λ_0, λ_1), velocity field (u_0, v_0) and normal temperature components (θ_{xx}, θ_{yy} and θ_{zz}) in the axisymmetric problem are exactly coincident with those resulting from the Laplace integration of the F–P equation (given in (27) and (34)). It is therefore likely that analytical solutions for β, p and q exist and, moreover, that they are identical to the Laplace results given in (34*b*), (35). These coincidences together with the excellent agreement found earlier between the exact solutions and the Laplace integrals imply that the hypersonic theory in the near-axis approximation is remarkably accurate.

The starting behaviour of p, q and β can be obtained by expanding all the known functions involved in (39f–h) in powers of s, retaining only the leading terms and trying for p-, q- and β-solutions of the form $p = p_0 s^{p_1}$; $q = q_0 s^{q_1}$ and $\beta = b_0 s^{b_1}$. When $\alpha = 0$ one obtains

$$p = \frac{1}{1+\delta}\left(\tfrac{4}{3}(1+\phi)-2\right), \quad q = \frac{2}{(1+\delta)s^2}, \quad \beta = \frac{5}{3(1+\delta)}.$$

In dimensional variables, for $\alpha = 0$:

$$u = U_0\left[1-\frac{\delta}{1+\delta}\frac{x}{U_0 \tau}+\frac{kT_b}{m_p U_0^2}\{\tfrac{4}{3}(1+\phi)-2\}-2\frac{y^2}{x^2}+O(x^2, y^4)\right], \tag{41a}$$

$$\boldsymbol{T} = \frac{T_b}{U_0 \tau}(2x\boldsymbol{e}_x\boldsymbol{e}_x+\tfrac{1}{2}x\boldsymbol{e}_y\boldsymbol{e}_y+\tfrac{5}{3}y(\boldsymbol{e}_x\boldsymbol{e}_y+\boldsymbol{e}_y\boldsymbol{e}_x)+O(x^2, y^2)). \tag{41b}$$

These results can also be derived from the Vlasov solution (24) by expansion in powers of θ, in the limit where $\theta \approx y/x \ll 1$.

In the case $\alpha \neq 0$, the results are $q = 0$, $\beta = \alpha/(s(1+\delta))$ (meaning that T_{xy} departs from its original zero value at the source as $T_0 y/x$), while the determination of p requires going one further step in the s-expansion and has not been carried out.

As an alternative path to the same conclusions it can be shown that the HH system (36), has a similarity solution in terms of the variable $\xi = y/\{\epsilon x^{(3-\phi)/2}\}$ close to the source. This feature permits (36) to be written as a set of ordinary differential equations in terms of ξ. The results are coincident with the above solution.

3. Two-dimensional stagnation-point flow

As an example of application of the HH equations, the case when particles move in a background gas with a linear flow field is considered. This is a logical extension of the previous example, though the coverage will be less thorough than before and will be restricted to the two-dimensional geometry. The preceding example illustrated a situation with no spatial gradients in the fluid driving fields T and U, where all the non-equilibrium could be ascribed to the injection conditions. In the present problem, non-equilibrium arises owing to the velocity gradients in the background gas.

3.1. *Results from the kinetic solution*

Consider two opposed jets, with axis $y = 0$ and symmetrical with respect to the plane $x = 0$. If viscous effects are ignored, the stagnation region where the two jets meet can be assumed to have a locally linear flow pattern. In the two-dimensional case, the carrier gas velocity field can therefore be described by

$$U = \omega(-x, y)$$

(see figure 2 in Fernández de la Mora 1982 for a sketch of the flow field). The temperature of the carrier gas is assumed uniform and equal to T. In the symmetric problem, particles are injected from a constant y-independent source, in equal amounts at $x \rightarrow \pm\infty$; in the non-symmetric problem, particles are injected only at one side, $x \rightarrow \infty$. This is a model reasonably close to reality if the nozzle throat is wide enough compared to the size of the stagnation region.

Fenández de la Mora (1982) found a special solution for this problem closely related to that given by Kramers (1940) for particles in a parabolic potential field. The solution is restricted to relatively slow decelerations, that is, for flow times $\omega^{-1} > 4\tau$. This condition can be expressed as $S < \frac{1}{4}$ (subcritical flows) where $S = \omega\tau$ is the Stokes number. For $S = \frac{1}{4}$, inertia dominates the flow and this solution breaks down. In the subcritical case it can be shown (Fernández de la Mora 1982) that the following hydrodynamic relations are exactly satisfied (under the y-independent seeding assumption):

$$U_p \equiv (u_p, v_p) = (-a(\omega x + D\lambda_{p,x}), b\omega y), \tag{42a}$$

$$T_{pxx} = T(1 - a\tau u_{p,x}), \tag{42b}$$

$$T_{pxy} = 0, \tag{42c}$$

$$T_{pyy} = bT, \tag{42d}$$

$$q_{pxyy} = q_{pxxy} = q_{pyyy} = 0, \tag{42e}$$

$$q_{pxxx} = -\tfrac{1}{2}\rho_p \frac{k}{m_p} Da\, T_{pxx,x}, \tag{42f}$$

where $a = [1-(1-4S)^{\frac{1}{2}}]/2S$, $b = [-1+(1+4S)^{\frac{1}{2}}]/2S$ and the density field is a function of x satisfying the following equation:

$$\frac{D}{\omega}\rho_{p,xx} + x\rho_{p,x} + \frac{a-b}{a}\rho_p = 0. \tag{43}$$

The equation for the heat flux can be written in the form $q_{pxxx} = -\lambda_c T_{pxx,x}$ where λ_c is a conductivity coefficient, which in analogy to the Chapman–Enskog expression can be written as

$$\lambda_c = C\frac{K}{m_p}\rho_p Da,$$

where the proportionality constant $C = \frac{1}{2}$ is related in the usual form to the dimensionless numbers of Schmidt (Sc) and Prandtl (Pr):

$$C = \frac{\gamma}{\gamma - 1} Sc\, Pr.$$

In problems under the Fokker–Planck assumptions, $Sc = \frac{1}{2}$ and $Pr = \frac{2}{3}$, while γ takes the value 3 in non-equilibrium situations, as will be illustrated in a later discussion.

From (43), $\rho_p = \rho_p(\xi)$ where $\xi = x(\omega/D)^{\frac{1}{2}}$. Consequently, new dimensionless variables can be introduced:

$$u = \frac{u_p}{(D\omega)^{\frac{1}{2}}}, \quad v = \frac{v_p}{(D\omega)^{\frac{1}{2}}}, \quad \eta = \frac{y}{(D/\omega)^{\frac{1}{2}}}, \quad \theta_{xx} = \frac{T_{pxx}}{T}, \quad \theta_{yy} = \frac{T_{pyy}}{T}$$

and the corresponding equations become

$$\lambda'' + \lambda'^2 + \xi\lambda' + \frac{(a-b)}{a} = 0, \tag{44a}$$

$$u = -a(\xi + \lambda'), \quad v = b\eta, \tag{44b}$$

$$\theta_{xx} = a(1 + Sa\lambda''), \quad \theta_{xy} = 0, \quad \theta_{yy} = b. \tag{44c}$$

The boundary conditions required to complete the integration of the above system

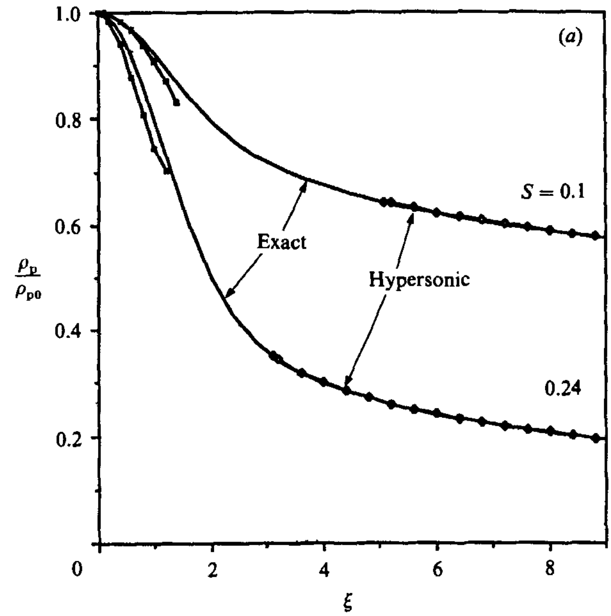

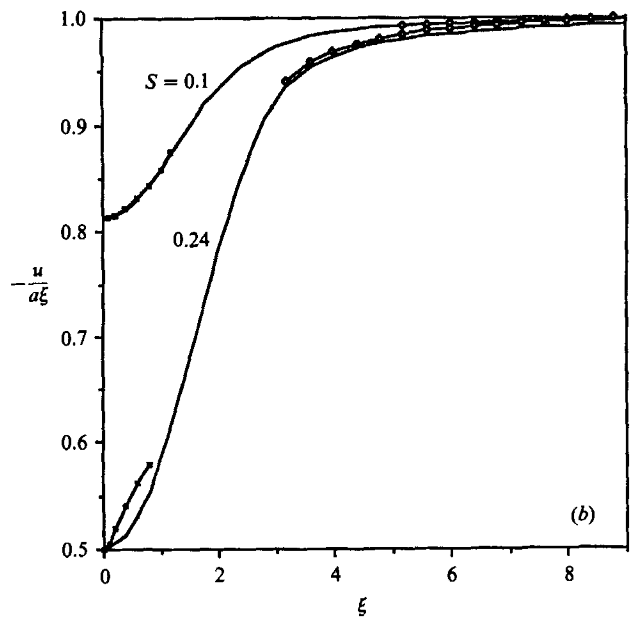

FIGURE 3 (a, b). For caption see facing page.

of equations are provided in the symmetric problem by symmetry considerations at the stagnation plane:

$$\text{at} \quad \xi = 0, \quad \lambda = 0, \quad \lambda' = 0, \quad \theta_{xx} = 1 + Sab, \quad u' = -b.$$

For large ξ the far-field solution is obtained:

$$\lambda' = -(a-b)/a\xi, \quad u = -a\xi, \quad \theta_{xx} = a.$$

In the non-symmetric problem, particles are injected only at one side of the

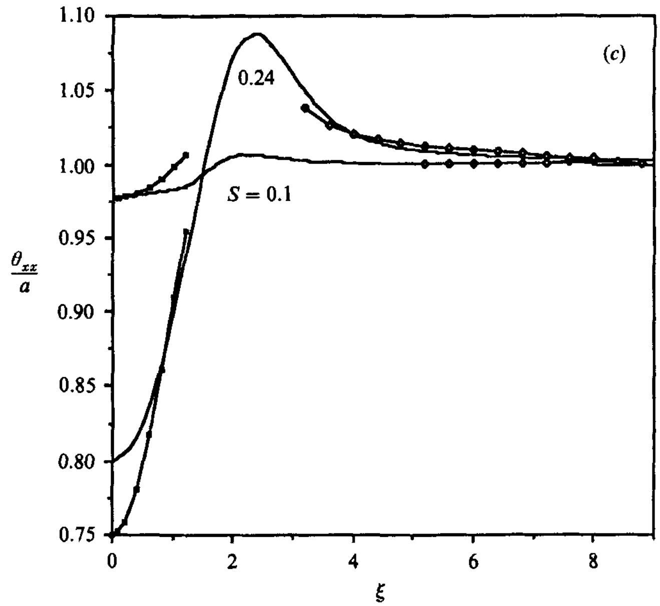

FIGURE 3. Stagnation point: particle hydrodynamic magnitudes in the symmetric problem ((*a*) density: ρ_p/ρ_{p0}; (*b*) axial velocity: $-u/(a\xi)$, and (*c*) axial temperature: θ_{xx}/a) as a function of ξ, for $S = \omega\tau = 0.1$ and 0.24. The kinetic solution of Fernández de la Mora (1982) is represented as a continuous line; also indicated is the numerical solution of the HH equations, starting in the far field for $Ma_p > 1$ ($\diamond$) and the local expansion around $\xi = 0$ of the HH equations ($\blacksquare$).

stagnation plane ($\xi > 0$) and they penetrate to the other side by diffusion and inertia against the mean motion of the host fluid flow. At this side, and far enough from the stagnation plane the gradients of density are large so that (43) becomes

$$\rho_{\xi\xi} + \xi\rho_\xi = 0,$$

from which the asymptotic behaviour as ξ tends to $-\infty$ for the non-symmetric case is obtained:

$$\rho \sim \operatorname{erfc}(-\xi/\surd 2), \quad \lambda' = \left(\frac{2}{\pi}\right)^{\frac{1}{2}} \frac{\exp(-\xi^2/2)}{\operatorname{erfc}(-\xi/\surd 2)}, \quad u = \frac{a}{\xi}, \quad \theta = 1 + \frac{Sa}{\xi^2}.$$

These expressions are used to start the integration of (36) at as sufficiently large and negative ξ in the non-symmetric problem.

3.2. *Hypersonic (HH) solution*

Equations (6)–(8) can be written in full as follows (using the normalization introduced in §3.1):

$$u\lambda_\xi + v\lambda_\eta + u_\xi + v_\eta = 0, \tag{45a}$$

$$S(uu_\xi + vu_\eta) + \theta_{xx}\lambda_\xi + \theta_{xy}\lambda_\eta + \theta_{xx,\xi} + \theta_{xy,\eta} + \xi + u = 0, \tag{45b}$$

$$S(uv_\xi + vv_\eta) + \theta_{xy}\lambda_\xi + \theta_{yy}\lambda_\eta + \theta_{xy,\xi} + \theta_{yy,\eta} - \eta + v = 0, \tag{45c}$$

$$S(u\theta_{xx,\xi} + v\theta_{xx,\eta} + 2\theta_{xx}u_\xi + 2\theta_{xy}u_\eta) + 2(\theta_{xx} - 1) = 0, \tag{45d}$$

$$S(u\theta_{yy,\xi} + v\theta_{yy,\eta} + 2\theta_{xy}v_\xi + 2\theta_{yy}v_\eta) + 2(\theta_{yy} - 1) = 0, \tag{45e}$$

$$S(u\theta_{xy,\xi} + v\theta_{xy,\eta} + \theta_{xx}v_\xi + \theta_{xy}(v_\eta + u_\xi) + \theta_{yy}u_\eta) + 2\theta_{xy} = 0. \tag{45f}$$

In the y-independent case it can easily be checked that ($45c, e, f$) are satisfied by

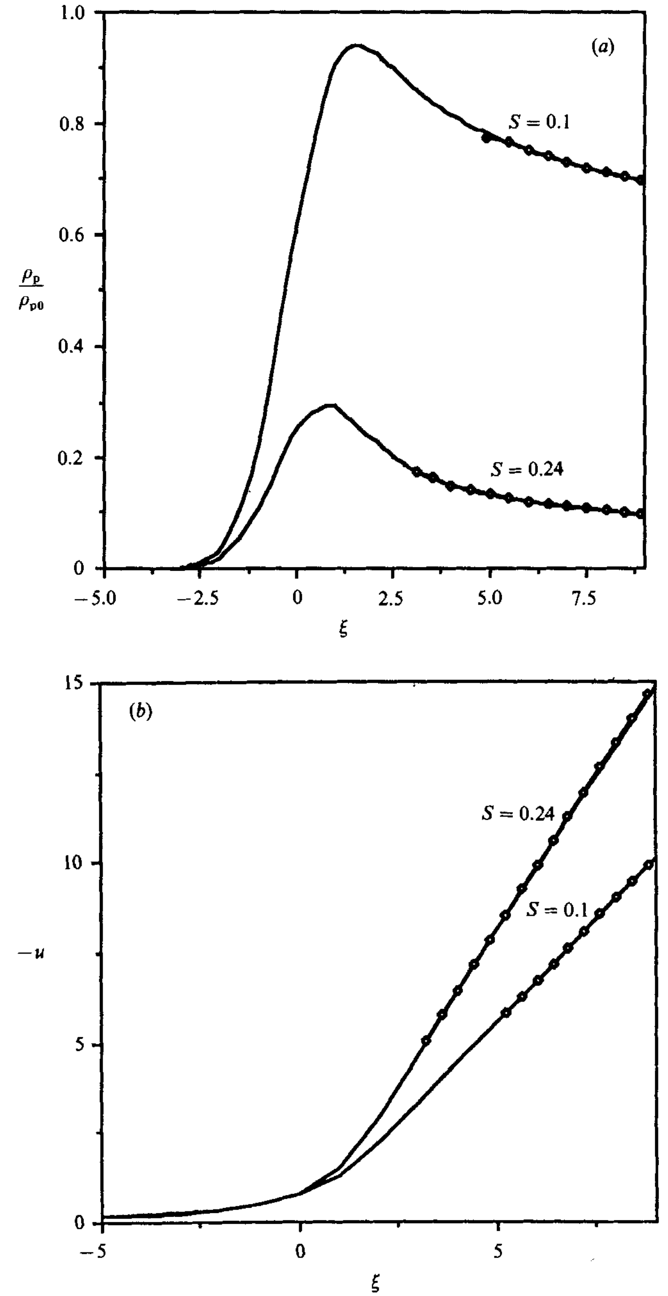

FIGURE 4(a, b). For caption see facing page.

making $v = b\eta$, $\theta_{xy} = 0$, $\theta_{yy} = b$ (using the definition of b, $Sb^2+b-1 = 0$) while the remaining equations become

$$u\lambda' + u' + b = 0, \tag{46a}$$

$$Suu' + \theta_{xx}\lambda' + \theta'_{xx} + \xi + u = 0, \tag{46b}$$

$$S(u\theta'_{xx} + 2\theta_{xx}u') + 2(\theta_{xx} - 1) = 0. \tag{46c}$$

If the exact solution (44a–c) is inserted here, the first two equations (continuity and

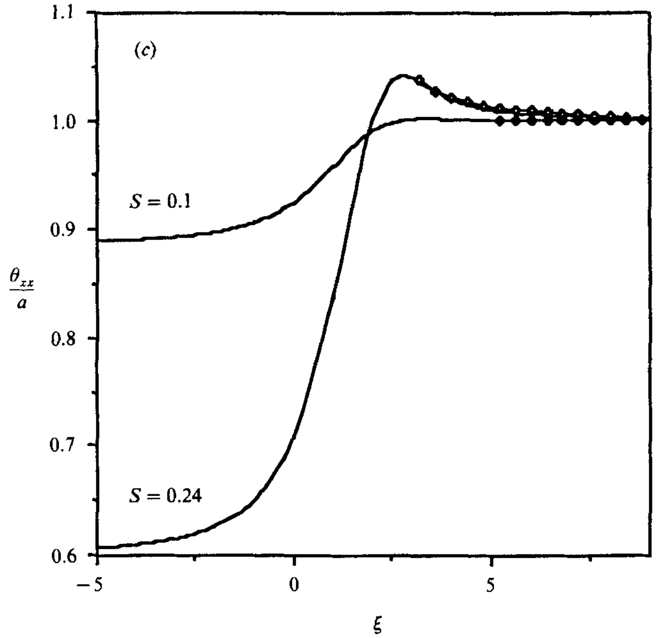

FIGURE 4. Stagnation point: particle hydrodynamic magnitudes in the non-symmetric problem ((*a*) density: ρ_p/ρ_{p0}; (*b*) axial velocity: $-u$, and (*c*) axial temperature: θ_{xx}/a) as a function of ξ, for $S = 0.1$ and $S = 0.24$. The kinetic solution of Fernández de la Mora (1982) is represented as a continuous line; also indicated is the numerical solution of the HH equations, starting in the far field, for $Ma_p > 1$ ($\diamond$).

momentum) are exactly satisfied, while a non-zero remainder is obtained in (46*c*). This is consistent with the method of truncation used to obtain (46) where the heat flux has been dropped in the energy equation. Equations (46) may be cast in matrix form

$$\boldsymbol{A} \cdot \boldsymbol{\omega}' = \boldsymbol{b}, \tag{47a}$$

$$\boldsymbol{A} = \begin{pmatrix} u & 1 & 0 \\ \theta_{xx} & Su & 1 \\ 0 & 2S\theta_{xx} & Su \end{pmatrix}; \quad \boldsymbol{b} = \begin{pmatrix} -b \\ -(\xi+u) \\ 2(1-\theta_{xx}) \end{pmatrix}; \quad \boldsymbol{\omega} = \begin{pmatrix} \lambda \\ u \\ \theta_{xx} \end{pmatrix} \tag{47b–d}$$

The determinant of $\boldsymbol{A}$ is $Su(Su^2-3\theta_{xx})$, so that the problem is singular for $u = 0$ (stagnation plane in the symmetric case) and for $u = \pm(3\theta_{xx}/S)^{\frac{1}{2}}$. The latter singularity is associated with a sonic point $Ma_p = |U_p|/c = 1$, where $c = (\gamma k T_{xx}/m_p)^{\frac{1}{2}}$ with $\gamma = 3$. Using the far-field solution, the sonic point can be approximately located at $\xi_s = (3a/S)^{\frac{1}{2}}$. Integration of (47*a*) is started in the far field (large positive ξ) and proceeds downstream, in the opposite direction as in the kinetically derived (44). However, the numerical integration becomes singular at the sonic point. Beyond the sonic point, the nature of the system of equations changes, and an initial-value condition is not sufficient to define the solution (both singular points $u = \pm(3\theta_{xx}/S)^{\frac{1}{2}}$, $u = 0$ are unstable nodes in the subcritical case $S < \frac{1}{4}$).

Figures 3 and 4 show profiles of ρ, u, θ_{xx} as a function of ξ in the symmetric and non-symmetric problem for two values of the inertia parameter ($S = 0.1$, $S = 0.24$). The exact solution is compared to the hypersonic results in the supersonic region, and it can be observed that even in the vicinity of the sonic point, a good agreement exists. An expansion of the HH equations around $\xi = 0$ in the symmetric case can be carried out to compare both solutions inside the subsonic region.

In the local HH solution (plotted up to three terms of expansion in figure 3)

$$\lambda = -\tfrac{1}{2}A\xi^2 \ldots, \quad u = -b\xi + \tfrac{1}{3}bA\xi^2 \ldots, \quad \theta_{xx} = \frac{1}{1-Sb} + \frac{2S^2b^3}{1-4bS}\xi + \ldots, \tag{48}$$

where $A = 2Sb^2(1-2bS)(1-bS)/(1-4bS)$. On the other hand, the exact expansions are

$$\lambda = \frac{(b-a)\,\xi^2}{2a}\ldots, \quad u = -b(\xi + \tfrac{1}{3}(1-b/a)\,\xi^3 + \ldots), \quad \theta_{xx} = 1 + Sab + bS(a-b)\,\xi^2 + \ldots. \tag{49}$$

If the a and b terms are expanded in powers of S around $S = 0$, (48) and (49) are seen to have a coincident initial behaviour:

$$\lambda = -S(1-S+\ldots)\,\xi^2 \ldots, \quad u = -b\xi + \tfrac{2}{3}bS(1-S+\ldots)\,\xi^3, \quad \theta_{xx} = 1 + S \ldots + 2S^2\xi^2.$$

Discrepancies therefore arise with increasing values of S.

An alternative method of solution for the HH equations with the clear advantage of holding throughout the whole range of velocities (subsonic as well as supersonic) consists in using a perturbative expansion in powers of S. Let $u = u_0 + Su_1 + \ldots$, $\theta_{xx} = \theta_0 + S\theta_1 + \ldots$, $\lambda = \lambda_0 + S\lambda_1 + \ldots$. Upon substitution, a sequence of equations is obtained:

$$u_0\lambda_0' + u_0' + b = 0, \tag{50a}$$

$$\lambda_0' + \xi + u_0 = 0, \tag{50b}$$

$$\theta_0 = 1; \tag{50c}$$

$$u_0\lambda_1' + u_1\lambda_0' + u_1' = 0, \tag{51a}$$

$$u_0u_0' + \lambda_1' + \theta_1\lambda_0' + \theta_1' + u_1 = 0, \tag{51b}$$

$$\theta_1 = -u_0' \tag{51c}$$

which can easily be solved with the same starting conditions used in the integration of (44a–c). As shown in figure 5(a), the convergence of the sequence of equations (50), (51), ... is fast and the agreement with the exact solution is very good in the case of $S = 0.1$. As S grows (see figure 5(b), for $S = 0.24$) the convergence becomes slower, and the expansion diverges for $S \geqslant \frac{1}{4}$.

Finally, some discussion is required on the validity of the HH equations. According to (51c), the heat flux which has been dropped out from (5) has the following relative value with respect to other terms of the equation:

$$\frac{q_{\mathrm{p}xxx}}{P_{\mathrm{p}xx}U_{\mathrm{p}}} = -\frac{Sa\lambda'''}{(\xi+\lambda')(1+Sa\lambda'')}.$$

In the far field, this ratio is of the order of $S\xi^{-4}$, that is, of S^3Ma^{-4}, so that provided that the Mach number is sufficiently large, the heat flux is negligible. In the subsonic region, the heat flux can also be neglected when the Stokes number is sufficiently small, or, alternatively, in the case of small temperature gradients $((D/T_{\mathrm{p}xx}U_{\mathrm{p}})/\mathrm{d}T_{\mathrm{p}xx}/\mathrm{d}x) \ll 1)$. Therefore, the validity of our truncation responds in the subsonic region to different physical reasons. No longer is it due to the prevalence of convection over conduction as a vehicle for energy transport, but to the vicinity to equilibrium conditions, on account of which viscous and heat conduction effects

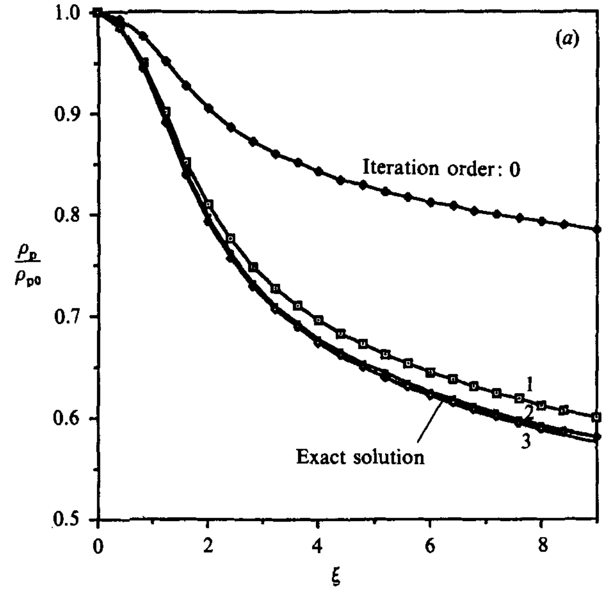

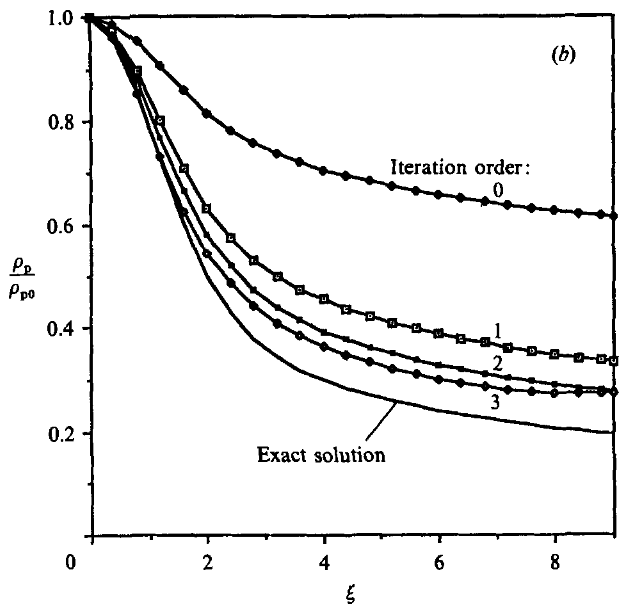

FIGURE 5. Particle density (ρ_p/ρ_{p0}) as obtained from a perturbative solution of the HH equations in powers of S ((*a*) $S = 0.1$ and (*b*) $S = 0.24$) in the symmetric stagnation point problem. The kinetic solution is plotted using a continuous line, and the different HH approximations (◆, order zero; ⊡, order one; ■, order two: ◇, order three).

become unimportant. The increasing importance of conduction effects as S grows can be observed in the figure.

In conclusion, the HH equations are surprisingly accurate up to the sonic point for values of S of order unity and also fairly accurate even down to zero velocity for small values of S. Not atypically, the theory functions well beyond its expected region of validity for this problem.

4. Conclusions

In the present paper, a systematically truncated set of hydrodynamic equations is used which differs from previous hypersonic formulations in going beyond the deterministic level by retaining the pressure term in the particle momentum equation. A hydrodymamic description of Brownian motion can thus be achieved in a wide range of far-from-equilibrium problems. The examples chosen are representative because they cover separately the case of injection non-equilibrium, originating at a boundary (source expansion problem) and the case of bulk non-equilibrium, due to non-uniformities in the background gas (stagnation point problem). The agreement between kinetic and hydrodynamic predictions is very good for all circumstances tested, including several not clearly supersonic. Hence the HH equations provide an effective tool to attack hydrodynamically a wide range of non-equilibrium Brownian motion problems whose direct kinetic solution would be extremely demanding computationally. The exact solutions developed here for the F–P equation should provide a useful standard against which to test other approximate theories.

We have benefited greatly from discussions with Dr R. Fernández-Feria and Dr J. O'Brien. This work has been supported by the National Science Foundation Grant CBT-86-12151 and the US Department of Energy Grant DE-FG02-87ER14550. One of the authors (P. R. C.) was funded by the US–Spanish Joint Committee for Cultural and Educational Cooperation. This work was completed at the Spanish Open University (UNED, Madrid; Departamento de Física Fundamental).

REFERENCES

Chandrasekhar, S. 1943 *Rev. Mod. Phys.* **15**, 1.

Edwards, R. M. & Cheng, H. K. 1966 *AIAA J.* **4**, 1556.

Einstein, A. 1908 *Z. Elektrochem.* **14**, 251.

Erdelyi, A. 1956 *Asymptotic Expansions*, p. 29. Dover.

Fernández de la Mora, J. 1982 *Phys. Rev.* A **25**, 1108.

Fernández de la Mora, J. & Fernández-Feria, R. 1987 *Phys. Fluids* **30**, 748.

Fernández de la Mora, J. & Riesco-Chueca, P. 1988 *J. Fluid Mech.* **195**, 1.

Fernández de la Mora, J. & Rosner, D. E. 1982 *J. Fluid Mech.* **125**, 459.

Fernández-Feria, R. 1989 *Phys. Fluids* A **1**, 474.

Fernández-Feria, R. & Fernández de la Mora, J. 1987*a* *J. Fluid Mech.* **179**, 21.

Fernández-Feria, R. & Fernández de la Mora, J. 1987*b* *J. Statist. Phys.* **48**, 901.

Freeman, N. C. 1967 *AIAA J.* **5**, 1696.

Freeman, N. C. & Grundy, R. E. 1968 *J. Fluid Mech.* **31**, 723.

Friedlander, S. K. 1977 *Smoke, Dust and Haze*. Wiley.

Gupta, D. & Peters, M. H. 1986 *J. Colloid Interface Sci.* **110**, 286.

Hamel, B. B. & Willis, D. R. 1966 *Phys. Fluids* **9**, 829.

Harris, W. L. & Bienkowski, G. K. 1970 *Phys. Fluids* **14**, 2652.

Kramers, H. A. 1940 *Physica (Utrecht)* **7**, 284.

Menon, S. V. G., Kumar, V. & Sahni, D. C. 1986 *Physica* **151 A**, 63.

Nguyen, T. K. & Andres, R. P. 1981 In *Rarefied Gas Dynamics*, vol. 74, p. 627. AIAA.

O'Brien, J. 1990 *J. Colloid Interface Sci.* **134**, 497.

Resibois, P. & DeLeener, M. 1977 *Classical Kinetic Theory of Fluids*. Wiley-Interscience.

RIESCO-CHUECA, P., FERNÁNDEZ-FERIA, R. & FERNÁNDEZ DE LA MORA, J. 1986 In *Rarefied Gas Dynamics* (ed. V. Boffi & C. Cercignani), p. 283. Stuttgart: Teubner.

WANG CHANG, C. W. & UHLENBECK, G. E. 1970 In *Studies in Statistical Mechanics* (ed. J. de Boer & G. E. Uhlenbeck), vol. V, pp. 89–92. North Holland.

WILLIS, R. & HAMEL, B. B. 1967 In *Rarefied Gas Dynamics* (ed. J. Brundin), p. 827. Academic.